D. Ceglarek*
Research Assistant.
Associate Mem. ASME

J. Shi
Research Fellow.
Associate Mem. ASME

S. M. Wu
Anderson Professor of Technology.
Fellow ASME

Department of Mechanical Engineering,
The University of Michigan,
Ann Arbor, MI 48109

A Knowledge-Based Diagnostic Approach for the Launch of the Auto-Body Assembly Process

This paper is the first attempt to implement a knowledge-based diagnostic approach for the auto-body assembly process launch. This approach enables quick detection and localization of assembly process faults based on in-line dimensional measurements. The proposed approach includes an auto-body assembly knowledge representation and a diagnostic reasoning mechanism. The knowledge representation is comprised of the product, tooling, process, and measurement representations in the form of hierarchical groups. The diagnostic reasoning performs fault diagnostic in three steps. First, an initial statistical analysis of measurement data is performed. Next, the Candidate Component and Candidate Station with the hypothetical fault are searched. Finally, the fault symptom is identified and the root cause is suggested. Two case studies are presented to demonstrate the implementation of the proposed method.

1 Introduction

In the automotive body assembly process, launch time is defined as the time between installation of the complete tooling equipment on the plant floor and the beginning at full scale production. The most time consuming part of the assembly process launch is verification and correction of faults related to tooling design and tooling installation. Therefore, efficient diagnostic of the assembly process is essential during launch time.

In recent years, in-line measurement gages (Optical Coordinate Measurement Machines—OCMMs) have been used to measure auto-body dimensions. OCMMs allow 100 percent measurement of products and therefore, are capable of providing tremendous information about product quality and the assembly process which challenge current diagnostic approaches. Based on in-line dimensional measurements, Hu and Wu (1992) proposed a diagnostic method applying a multivariate statistical technique—Principal Components Analysis (PCA). PCA has been used successfully in reducing variation of the body assembly process, resulting in a significant quality improvement.

Such multivariate approaches focus on statistical input-output relationship. They enable one to analyze large numbers of variables that can affect product quality. However, these approaches center mostly on the ability to identify a process model, making no use of knowledge of the product structure and the tooling system. Thus, they are merely statistical tools for variation reduction rather than systematic approaches to the diagnostic of an assembly process.

Knowledge of the product and assembly process should be actively integrated with statistical analyses in order to develop an efficient diagnostic approach. Some recent research has investigated the integration of statistical methods with knowledge-based techniques to provide enhanced decision support capabilities (Schwarz and Lu, 1992). Dessouky et al. (1987) successfully applied decision tree analysis, supported by time series modeling and factorial design experimentation techniques, to diagnose process quality. Dooley and Kapoor (1990a, 1990b) proposed an enhanced quality evaluation system for continuous manufacturing processes. They developed a rule base to classify various types of signal changes such as mean and variance.

Knowledge-based diagnostic systems have been used in manufacturing processes. Becker et al. (1989) proposed a diagnostic system which involved implementing a knowledge-based approach in the form of a model-based representation. The system explicitly represents the relationship between components and the order of process steps, as well as what the process steps are designed to accomplish and what causes them to fail. An on-line model-based diagnostic system was proposed by Isermann and Freyermuth (1991). Knowledge of the process is represented in the form of heuristic knowledge (fault trees) and analytical knowledge (input-output relations). Though there is evidence of successful implementation of knowledge-based approaches in diagnostic, yet very little research has been done with regards to investigation of these approaches during the launch of a new auto-body assembly process.

This paper is the first attempt to develop a knowledge-based diagnostic approach for the launch of auto-body assembly. When launching a new process, pre-enumerated faults and identified case studies are unavailable. Therefore, an experience-based diagnostic technique used, for example, in classical rule-based systems such as MYCIN (Buchanan and Shortliffe, 1984) and DENDRAL (Buchanan and Feigenbaum, 1978) cannot be used in this application. Additionally, these systems

*Currently Research Fellow at the University of Michigan.

Contributed by the Production Engineering Division for publication in the JOURNAL OF ENGINEERING FOR INDUSTRY. Manuscript received Jan. 1993; revised Nov. 1993. Associate Technical Editor: S. Kapoor.

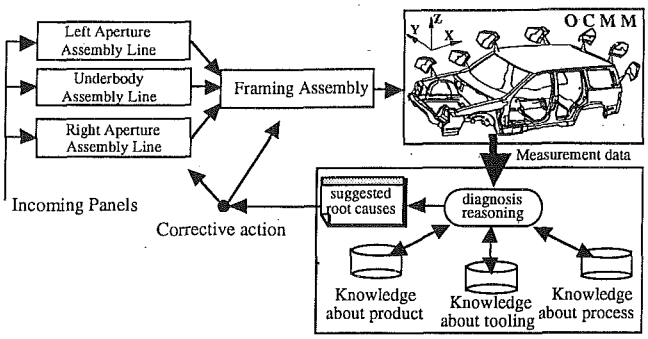

Fig. 1 A schematic diagram for knowledge-based diagnosis approach

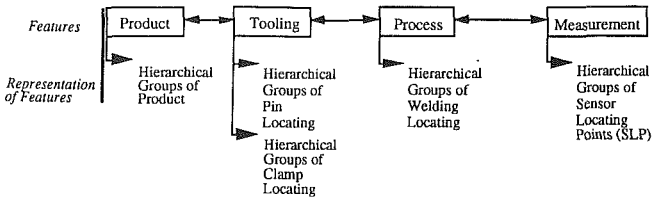

Fig. 2 Major features of auto-body assembly and their representation

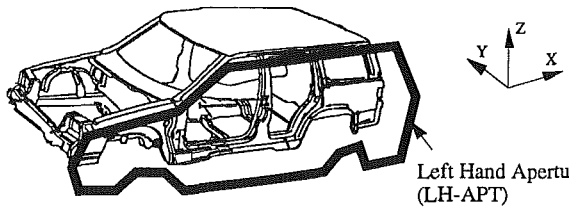

Fig. 3 Auto-body with marked LH-APT

were mainly heuristic with no direct support from the physics (deep system) of the domain. To overcome these limitations, Lu and Tcheng (1991) developed a layered model building process from a detailed mechanistic description of the task based on the domain physics.

In this paper, a systematic approach is proposed for knowledge-based diagnostic of the auto-body assembly process. A schematic diagram for knowledge-based diagnostic is shown in Fig. 1.

This paper is organized as follows: section 2 describes the knowledge representation of the product and the assembly tooling and process. Section 3 introduces diagnostic reasoning, which allows detection and location of dimensional faults. Section 4 presents two case studies demonstrating the implementation of the proposed approach.

2 Knowledge Representation

The knowledge representation presented here supports a novel approach to reasoning in the diagnostic of the auto-body assembly process. Instead of reasoning from experience based on previously solved case studies, relevant knowledge structures are built from key design features of the assembly process. In this study four features are taken into consideration in the knowledge representation for the assembly process diagnostic. These features include: knowledge of the product, of tooling, of process, and, of measurements. Figure 2 shows major features of the auto-body assembly and their representation using hierarchical groups. A detailed description of the features and their representations are summarized in the following sections.

2.1 Product Representation. A set of components and subassemblies is used to represent the auto-body in the form of Hierarchical Groups (HG) of the product. The component and subassembly groups are organized in order of their assembly sequences. Figure 3 shows the auto-body used in this research. The HG of the product showing details of the left hand aperture (LH-APT) is presented in Fig. 4. In the following discussion, the LH-APT is used as an example to explain the concept of the HG of the product.

The LH-APT consists of four layers (Fig. 4). Starting from the Aperture Complete (layer 3), the aperture is divided into two groups: the Aperture Outer Complete and the Aperture Inner Complete (layer 4). Then, for example, the Aperture Inner Complete is further divided into four groups (layer 5), each of which may be composed of subgroups. For instance, the rear quarter inner of layer 5 is further divided into three groups (layer 6). For simplicity, each component of the HG of the product will be represented as $C_{i,j}$, where i stands for the layer number and j represents the subassembly within the ith layer. Using this compact taxonomy represented by the HG, one can set up an exhaustive description of the product structure and of the assembly sequence. Additionally, assembly stations, marked as S_i ($i = 1, \ldots, 7$), are also presented in the HG of the product (Fig. 4).

In general, the HG of the product represents all components and intermediate subassemblies. Thus, the size and the scope of the HG depends on the complexity of the designed product and assembly process. For the auto-body studied in this paper, the whole HG of the product consists of 10 layers, 22 stations and 70 panels or subassemblies.

2.2 Representation of Tooling. Representation of tooling provides information about the method of holding subassemblies in the fixtures during the assembly process. Two representations were selected to describe tooling features: (*1*) Pin Locating Points (PLPs) and (*2*) Clamp Locating Points (CLPs). PLPs define the orientation of the subassemblies in the fixtures during the assembly process. CLPs describe the clamping tasks by using information about the location of the clamping points and their respective directions.

Nomenclature

$C_{i,j}$ = jth component in the ith layer
$C^c_{i,j}$ = jth component in the ith layer, when also a Candidate Component
$Cl_{i,j}(a)$ = jth Clamp Locating Point in the ith layer, controlling the a axis
CMI = Criterion of Mode Importance
$Corr^{k,l}_{i,j}(\bullet, *)$ = correlation between sensors $Sn_{i,j}(\bullet)$ and $Sn_{k,l}(*)$
CSS = Candidate Set of Sensors
$P_{i,j}(a, b)$ = jth Pin Locating Point in the ith layer, controlling the a and b axes
S_i = ith station in the assembly line
S^c_i = ith station in the assembly line, when also a Candidate Station
$Sn_{i,j}(\bullet)$ = jth Sensor Locating Point in the ith layer, controlling the $(\bullet)$ axis
T_c = correlation threshold
T_v = variation threshold
$Var_{i,j}(\bullet)$ = variation of sensor $Sn_{i,j}$ in the $(\bullet)$ axis
$W_{i,j}(a)$ = jth Weld Locating Point in the ith layer, controlling the a axis

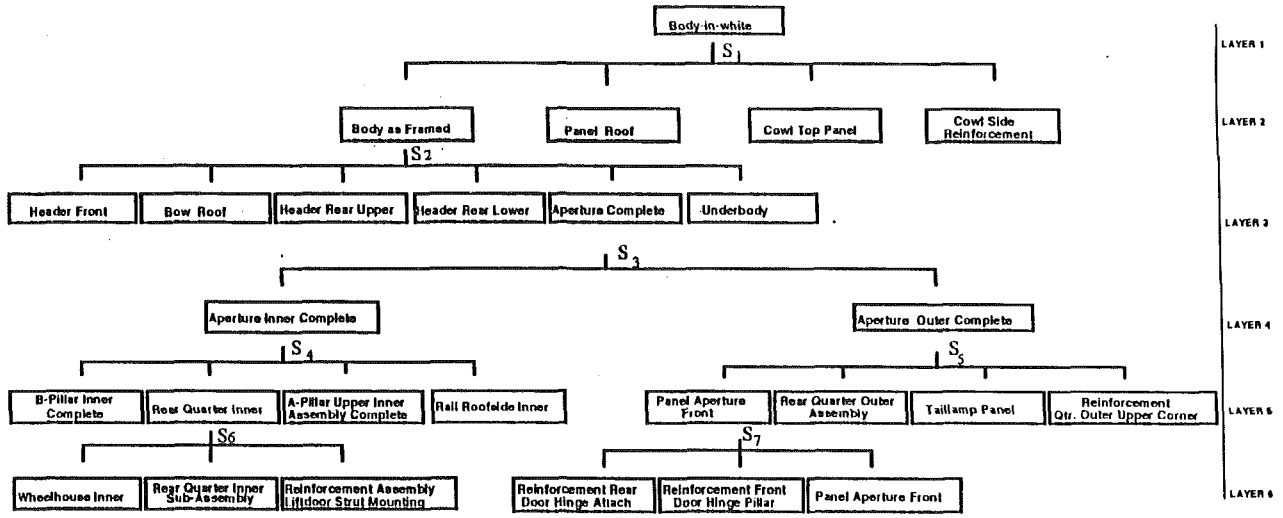

Fig. 4 Hierarchical Group of auto-body structure

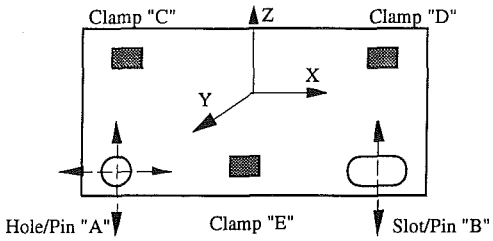

Fig. 5 Scheme of "3-2-1" principle for tooling design

In general, tooling design follows the "3-2-1" principle for a rigid body (Chou, 1992). Typically, two pins are used to orient the panel as shown in Fig. 5. In Fig. 5, pin A controls axes X and Z, and pin B controls axis Z. Three clamps C, D, and E control the Y axis.

Figure 6 shows three layers of hierarchical groups of PLPs in the LH-APT. The symbol $P_{n1,n2}(a, b)$ means the n_2th PLP on layer n_1, controlling the a and b axes. Axes a and b represent one of the $\{x, y, z\}$ directions each. It can be seen that the first group (layer 3) contains two PLPs: $P_{3,1}(x, z)$ and $P_{3,2}(z)$. In layer 4, two PLP groups can be found: $\{P_{4,1}(x, z), P_{4,2}(z)\}$ and $\{P_{4,5}(z), P_{4,4}(z), P_{4,3}(x, z)\}$. The other layers are treated in a similar manner.

A similar Hierarchical Group of the CLPs is used to represent clamps.

2.3 Representation of Process. The assembly process consists of a succession of tasks, each of which consists of joining subassemblies or panels to form a larger subassembly. The process starts with all panels separated and ends with all panels properly joined to form the whole auto-body. In this paper, the assembly process is comprised of joining operations in which panels are joined through spot welds. Location, directions and quality of the welding spots are the process features, that must be represented for the diagnosis. In the current analysis, the process is represented as the HG of Welding Locating Points (WLPs). The HG of WLPs describes the location and sequence of the individual welding spots on the components during assembly operations. The layout of the HG of WLPs is similar to that of the PLPs.

2.4 Measurement Representation. Currently, in-line OCMMs are located after each mean assembly operation, i.e. apertures, underbody and framing. The number of sensors depends on the complexity of the process. On average, 40–100 points are measured at each measurement station.

The measurements provide information about the location of measured points on the auto-body or subassemblies. In this paper a single representation, Sensor Locating Points (SLPs), was selected to describe the measurement feature. SLPs describe measurement information by giving the location of all sensors. Similarly, as with the PLP, CLP and WLP groups, the method of hierearchical groups was applied to represent measurements. Figure 7 shows layer 4 of the SLP groups in the LH-APT. In Fig. 7, the symbol $Sn_{n1,n2}(a, b, c)$ means the n_2th SLP located on the n_1th layer with measurements in the a, b and c axes, where a, b and c are one of the $\{x, y, z\}$ axes each. A single sensor may measure one, two or three axes. The selection of the sensor axes is based on the analysis of the critical dimensions of the auto-body. For example, in case of slot "B" (Fig. 5), z is the most important direction. The design purpose of this slot is to control the subassembly only in the z axis. The x axis is not critical and therefore not measured by the sensor.

3 Diagnostic Reasoning

The diagnostic reasoning provides automated assistance for the assembly process diagnosis. It was designed to detect the most severe fault at any given time. The reasoning scheme has three major steps (Fig. 8): (*1*) Problem identification—selection of Candidate Set of Sensors (CSS) by determining which sensors plausibly detect the hypothetical fault, (*2*) Problem analysis—determination of the Candidate Component (failing panel or subassembly) as well as Candidate Station (assembly station causing hypothetical fault) and (*3*) Root cause identification—detection of the fault symptom and its root cause. This procedure is based on the assumption that at any given time one fault occurs on one component.

3.1 Problem Identification. The objective of this phase is to select and classify measurement information in the form of the CSS set. It is comprised of two sub-tasks:

(*1*) *Selection of Measurement Information by Estimation of Data Variation.* After acquiring the data, the variation $Var_{i,j}(\bullet)$ for each sensor $Sn_{i,j}^{(t)}(\bullet)$ in axis $(\bullet)$ is calculated as:

$$Var_{i,j}(\bullet) = \frac{\sum_{m=1}^{N} (Sn_{i,j}^{(t-m+1)}(\bullet) - \bar{Sn}_{i,j}^{(N)}(\bullet))^2}{N-1} \quad (1)$$

where $t \geq N$ is the current number of produced auto-bodies, and $\bar{Sn}_{i,j}^{(N)}(\bullet)$ is an average of the last N measurements of sensor $Sn_{i,j}^{(m)}(\bullet)$, m is an auto body number, and $m \in [t - N + 1, t]$.

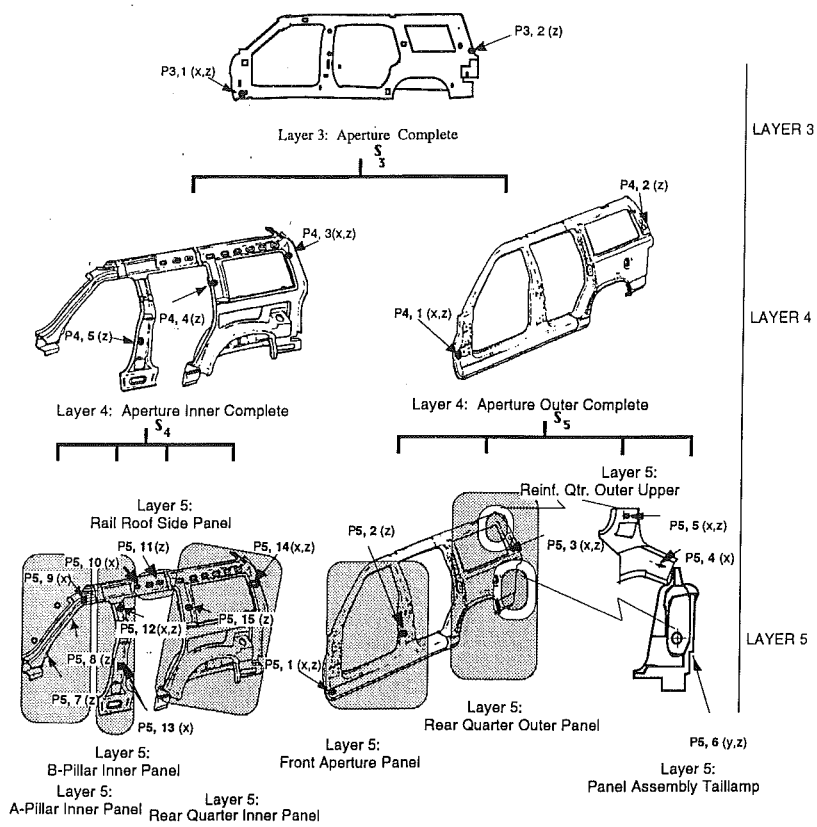

Fig. 6 Hierarchical Group of Pin Locating Points (PLP)

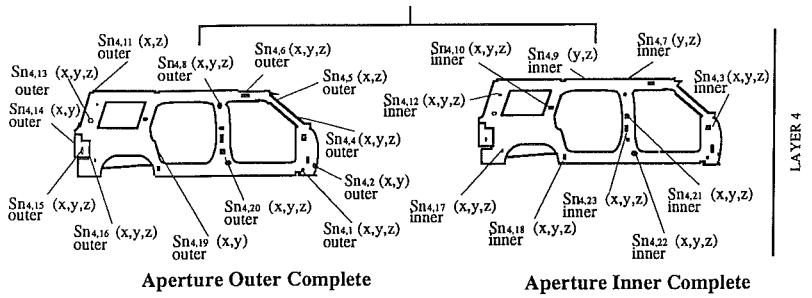

Fig. 7 Hierarchical Group of Sensor Locating Points

The presented diagnostic approach assumes detection of the faults one by one, from the most severe to the least. To concentrate the most severe fault, a variation threshold, T_v, is pre-set based on the percentile chart. The variation percentile chart is generated by plotting the 6-sigma value for each sensor, starting from the lowest to the highest one. In general, T_v is determined so that 70 percent of the inspected points fall below (Fig. 9). Therefore points shown on the percentile chart above T_v are focused during further diagnosis. T_v decreases when the overall variation of the product is reduced.

(2) Problem Classification Using Correlation Analysis. The diagnostic approach developed in this paper analyzes problems with a single root cause. In general, several independent root causes in the assembly process can lead to larger variation of the product, which may be reflected in many measurements. Therefore, an approach needs to be developed to classify these measurements based on a single root cause. The proposed approach is based on correlation analysis.

The correlation $Corr_{i,j}^{k,l}(\bullet, *)$, between sensors $Sn_{i,j}^{(t)}(\bullet)$ and $Sn_{k,l}^{(t)}(*)$ is calculated for all sensors with variance exceeding T_v as:

$$Corr_{i,j}^{k,l}(\bullet, *) = \frac{\sum_{m=1}^{N} (Sn_{i,j}^{(t-m+1)}(\bullet) - \overline{Sn}_{i,j}^{(N)}(\bullet))(Sn_{k,l}^{(t-m+1)}(*) - \overline{Sn}_{k,l}^{(N)}(*))}{\sqrt{\left[\sum_{m=1}^{N} [Sn_{i,j}^{(t-m+1)}(\bullet) - \overline{Sn}_{i,j}^{(N)}(\bullet)\right]^2 \left[\sum_{t=1}^{N} (Sn_{k,l}^{(t-m+1)}(*) - \overline{Sn}_{k,l}^{(N)}(*)\right]^2}} \quad (2)$$

The correlation threshold, T_c, is pre-set for the classification purpose. The correlation threshold is a second constraint in grouping measurements to achieve a single fault root cause. It is based on the assumption that measurements with large variation are strongly correlated if and only if their variation

is caused by the same root cause. $T_c = 0.7$ was selected according to the simulation studies done by Jolliffe (1972), where it is concluded that variables with correlation less than 0.7 contain less information than a single variable. The set of all sensors $Sn_{i,j}$ that exceeds T_v and T_c thresholds are defined as the Candidate set of sensors (CSS), i.e., let μ, χ be such that $Sn_{\mu,\chi}$ is a sensor with largest variation:

$$\text{CSS} = \{Sn_{k,l}(*) \mid (\text{Var}_{k,l}(*) > T_v) \ \& \ (Corr^{k,l}_{\mu,\chi}(\bullet, *) > T_c) \tag{3}$$

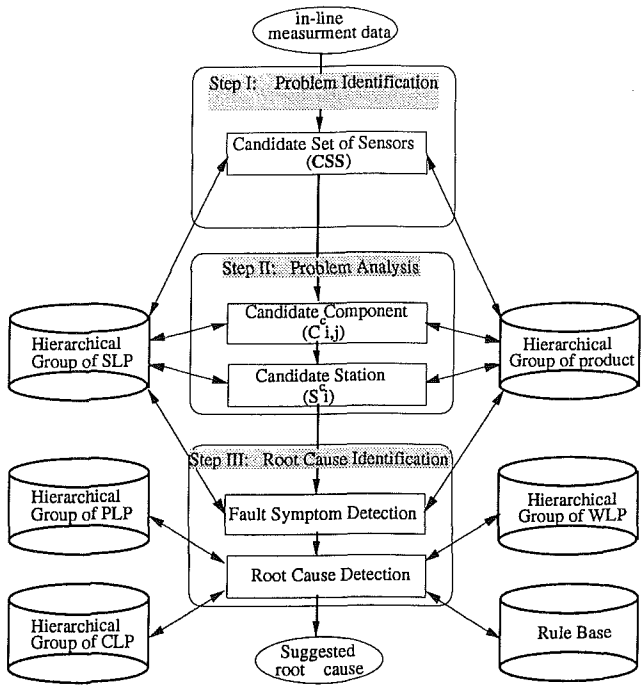

Fig. 8 Flow chart of diagnosis reasoning

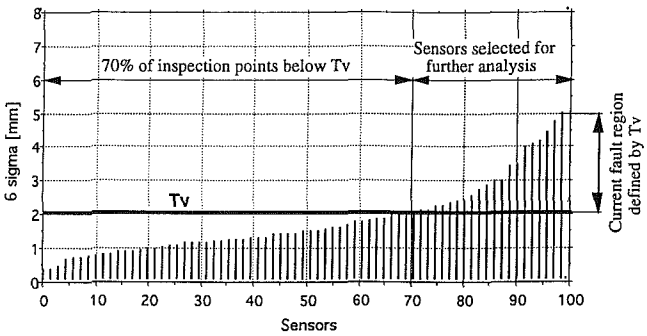

Fig. 9 Example of percentile chart used for Tv determination

3.2 Problem Analysis. This step localizes the fault based on information included in the CSS (subset of the HG of SLP) and the knowledge of the HG of the product. The problem is localized by mapping information about hypothetical faults represented by the selected sensors (CSS) onto components represented by the HG of the product. This mapping determines the faulty component of the auto-body, as well as an assembly station causing this fault. To realize this, two tasks are proposed:

(*1*) *Determination of the Candidate Component.* This task leads to determining components, referred to as Candidate Components, $C^c_{i,j}$, which manifest the symptom of the hypothetical fault. The proposed approach to determine Candidate Components is based on the general idea of hierarchical classification (Gomez and Chandrasekaran, 1981) and the following observations. In hierarchical classification, domain knowledge is organized as a hierarchical collection of categories, each of which contains knowledge that help in diagnosis of the unknown input data. Each category in this hierarchy represents a fault location in the system. More general fault locations are higher in the hierarchy, while more specific ones are lower in the structure (Chandrasekaran and Goel, 1988).

In the assembly system, represented by the HG of the product (Fig. 4), the fault occurrence during assembly can be thought of as bottom-up propagation, while their manifestation, shown by sensors, are analyzed in a top-down fashion. Top-down manifestation of the component fault defines not only the direction of the fault manifestation but also the resolution of fault location in the HG of the product (Fig. 10). The Candidate Component determination procedure operates on the analysis of individual components of the HG of the product by using information from the HG of SLP.

Currently, a common approach in similar situations involve applying techniques based on the known probability constraints imposed by the failure relations between components (Narayanan and Viswanadham, 1987). This diagnostic approach assumes a priori knowledge of some solved problems based on which probability constraints can be estimated. Another approach (Scarl et al., 1987) assumes a priori knowledge about all possible fault hypotheses. Scarl et al. (1987) present failure source location diagnostic, which is based on the hierarchical fault propagation model. It backtracks along all feasible fault propagation paths in the hierarchical structure of the system, starting from the components indicated to be faulty by alarms, and locates a set of components which may be the sources of failure in that structure. These approaches assume that failure relations between components, represented in the form of probabilities or fault propagation models, are known. The proposed approach of this paper relaxes this assumption in the following way.

The $C_{i,j} \subset$ (HG of the product) is said to be a Candidate Component $C^c_{i,j}$ if:

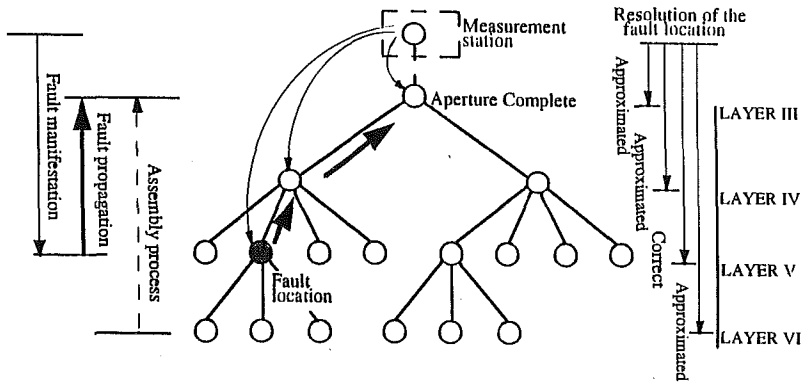

Fig. 10 Mechanism of fault propagation and manifestation in the HG of the product

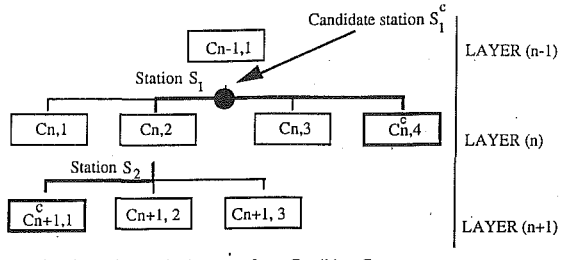

(a) Candidate station determination in the case of two Candidate Components

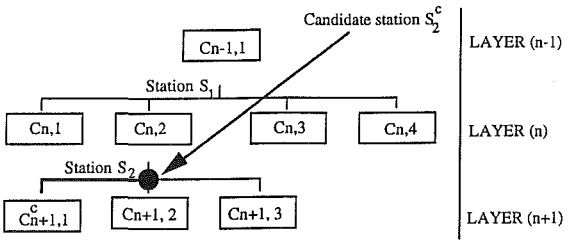

(b) Candidate station determination in the case of one Candidate Component

Fig. 11 Example scheme of the candidate station determination

$$\eta(C_{i,j}^c) = \left\{\frac{n_{i,j}^*}{n_{i,j}}\right\} = \text{maximum} \tag{4}$$

for all $C_{i,j}$ in the assembly path. The $n_{i,j}$ represents number of SLPs located on the $C_{i,j}$, and $n_{i,j}^*$ represents number of SLPs from CSS which are located on the $C_{i,j}$. An assembly path is a sequence of consecutive stations (not components). For example, for the aperture there are two assembly paths: (*1*) $S_3 \rightarrow S_4 \rightarrow S_6$, and (*2*) $S_3 \rightarrow S_5 \rightarrow S_7$ (Fig. 4).

The number of Candidate Components depends on the number of the assembly paths. The maximum η for one path is treated as a first approximation in the determination of Candidate Component. The proposed approach uses the number and location of the selected sensors (CSS) to determine the faulty component. It does not require any a priori knowledge about failure relations between components.

(*2*) *Determination of the Candidate Station.* This task determines the station where the hypothetical fault has occurred. This station is called Candidate Station S_i^c. Notice that the set of all stations, S_i, for nodes labeled from S_1 to S_7 in Fig. 4, represents a catalog of stations in the aperture assembly line.

The approach to determine the S_i^c is based on the information about $C_{i,j}^c$ and the HG of the product. The Candidate Station S_i^c is chosen to be the nearest station between two Candidate Components on the diagram of HG of the product. For example, the Candidate Station S_1^c shown in Fig. 11(*a*) as S_1, represents the first assembly station where the Candidate Components $C_{n+1,1}^c$ and the $C_{n,4}^c$ are assembled (welded) together. The bold line in Fig. 11(*a*) shows the search path of the S_1^c on the HG of the product structure, which can be interpreted as an assembly path of the Candidate Components $C_{n+1,1}^c$ and $C_{n,4}^c$. In case of more than two Candidate Components, each pair of the components is treated separately in the way described above. In case of the only one Candidate Component, the first station in the sequence of the assembly process that welds the Candidate Component to the subassembly is treated as the Candidate Station [Fig. 11(*b*)].

3.3 Root Cause Identification. The objective of the root cause identification is to map a symptom (product fault) into a root cause (assembly line fault). The root cause identification step is based on the previously determined: CSS, Candidate Component(s), Candidate Station, and is supported by statistical analysis. The root cause identification procedure is divided into two sub-tasks, namely, fault symptom detection and root cause detection.

(*1*) *Fault Symptom Detection.* Fault symptom detection is based on the Principal Component Analysis (PCA) (Jolliffe, 1986) and its objective is to describe the deformation of the Candidate Component $C_{i,j}^c$ causing the variation shown by measurement data. Here deformation means the dimensional deviation from the nominal values of any point located on the $C_{i,j}^c$. It might be a mislocation of the $C_{i,j}^c$ during subassembly, or the distortion of the panel due to a nonequalized welding gun or a shaky clamp.

The fault symptom detection step includes two sub-tasks: detection of the *Vector of deformation* and the *Area of deformation*. The Vector *of deformation* is a vector represented by directions and magnitude of variance for each sensor of the CSS.

The *Vector of deformation* is estimated using PCA. This analysis can be summarized as follows (Jolliffe, 1986; Hu and Wu, 1992):

Let $\mathbf{x}_i \in \Re^p$, $(i = 1, \ldots, n)$ represents n measurements with covariance matrix Σ. Each variable represents one sensor from the CSS set. The covariance matrix Σ is the matrix whose (i, j) element is the known covariance between the ith and jth element of $\mathbf{x}$.

Define $\mathbf{y}_i \in \Re^q$ and $q < p$, as transformation of $\mathbf{x}_i$'s such that $\mathbf{y}_i = \mathbf{B}^T\mathbf{x}_i$, $(i = 1, \ldots, n)$ here $\mathbf{B}$ is a $(p \times q)$ orthonormal matrix constructed as follows: let the kth column of $\mathbf{B}$ be the kth eigenvector of the covariance matrix Σ.

In other words, $\{\mathbf{y}_1, \ldots, \mathbf{y}_n\}$ are projections of $\{\mathbf{x}_1, \ldots, \mathbf{x}_n\}$ onto the q-dimensional eigenspace spanned by the q eigenvectors of Σ. In order to effectively use information from the Principal Component Analysis, an index Criterion of Mode Importance (CMI) is defined as:

$$\text{CMI}_i = 100\,\frac{\lambda_i}{\sum_{k=1}^{p}\lambda_k}\ (\%) \tag{5}$$

where λ_i indicates the ith eigenvalue calculated for covariance matrix Σ. CMI indicates the relative importance of principal components in terms of their variances (indicated by the eigenvalues) in comparison to the variances of the original variables. In our application, a criterion was set up at the level of $\omega = 80$ percent to account for the first two modes:

$$\text{CMI} = \sum_{i=1}^{2}\text{CMI}_i > \omega \tag{6}$$

It means, supposing that the first two modes contributed ω percent of the total variance, further analysis will continue. Otherwise, if more than two modes are significant T_c is increased and CSS is redefined. This procedure is based on the observation that it is much more difficult to find the root cause if more than two modes contribute to the overall variation of the correlated sensors.

The *Area of deformation* of the $C_{i,j}^c$ is defined in terms of the percentage of sensors located in the $C_{i,j}^c$ belong to the CSS set. If most of the sensors (heuristically set as $\eta = 75$ percent) in the $C_{i,j}^c$ belong to the CSS, it is assumed to be a *global symptom*. This means the Area of deformation is distributed throughout the whole component. Otherwise, it is assumed to be a *local symptom*.

(*2*) *Root Cause Detection.* Root cause detection starts when the detected fault symptom provides information about the direction and area of deformation. The four features chosen for our analysis, namely PLPs, CLPs, WLPs, and external interference, form a general class of parameters that explain the most common root causes of the faults occurring in the assembly process. The relationship between root causes and their corresponding symptoms are summarized in Table 1.

Table 1 Root cause—symptom relations table

Root causes		Fault symptoms	
Identification	Description	Direction of deformation	Area of deformation
2-way PLP 1-way PLP	• mislocation • worn out • loose • missing	X and Z Z (or X)	global
CLP	• not functioning • missing • not closing properly	Y	global
WLP	• unequalized welding gun • worn out tip • missing welding spot • malfunction of tip • dressing operation	Y	local (location of the WLP)
External interference		X, Y or Z	local

3.4 Summary of Diagnostic Reasoning. The following procedure shows the overall diagnostic reasoning:

(*1*) Select the Candidate Set of Sensors
- (*a*) Set T_v and T_c based on the quality level and experience. (in general, $T_c = 0.7$ is recommended);
- (*b*) Based on Eq. (3) and supported by Eqs. (1) and (2) select all sensors for which measurements exceed T_v and T_c. The selected sensors constitute the CSS set.

(*2*) Determine the Candidate Component $C^c_{i,j}$ [Eq. (4)] by mapping between the HG of the product and the HG of SLP.

(*3*) Determine the Candidate Station (Fig. 11) based on the $C^c_{i,j}$ with reference to the HG of product:
- *IF* (there is one Candidate Component = $C_{i,j}$)
- *THEN* (the first station in the sequence of the assembly process (HG of the product) that weld $C_{i,j}$ with the subassembly is called the Candidate Station S^c_i) [see Fig. 11(*b*)]
- *IF* (there are two Candidate Components: $C_{i,j}$ and $C_{l,k}$)
- *THEN* (the first station in the sequence of assembly process (HG of the product) that bring $C_{i,j}$ and $C_{l,k}$ together is called the Candidate station S^c_i) [see Fig. 11(*a*)]
- *IF* (there are more than two Candidate Components)
- *THEN* (each pair of components is treated separately in the way described above)

(*4*) Fault Symptom Detection
- (*a*) Vector of deformation based on the PCA and criterion CMI > 80 percent
- (*b*) Area of deformation [Eq. (4)]
  IF η > 75 percent *THEN* *global symptom*
  ELSE *local symptom*

(*5*) Root Cause Detection
- *IF* (direction of deformation is *X* or *Z*)
- *THEN* (suggested root cause is the PLP pin in Candidate Station S^c_i, (HG of PLP) the closest to the biggest element of the Vector of deformation)
- *IF* (direction of deformation is *Y*) & (Area of deformation = *global symptom*)
- *THEN* (suggested root cause is CLP in the Candidate Station S^c_i, the closest to the largest element of the Vector of deformation)
- *IF* (direction of deformation is *Y*) & (Area of deformation = *local symptom*)
- *THEN* (suggested root cause is the WLP in the Candidate Station S^c_i, the closest to the largest element of the Vector of deformation) OR (unidentified external interference close to the biggest element of the Vector of deformation)

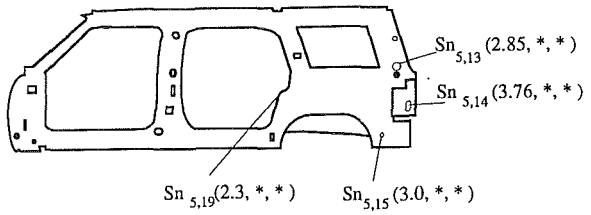

Fig. 12 Case study I-LH-APT scheme with marked elements of CSS

4 Case Studies

Two case studies are presented to illustrate the proposed diagnostic approach. The emphasis of these case studies is to demonstrate the applicability of the proposed approach during the launch of a new product in the assembly plant. The dimensional faults, which occurred during launch time, were caused by tooling faults, such as tooling design and tooling installation. Each case study is presented in four steps to illustrate the diagnostic procedure. Three of these steps are listed in section 3, and the last one is root cause verification and evaluation.

Case Study I: Aperture Variation in the X Axis. This case study illustrates diagnostic of a fault pertaining to tooling design. The correction of this fault involved redesigning of the tooling.

Step (1) Problem Identification

Task I First, constraints were specified in the form of the variation threshold, $T_v = 2.30$ mm, (6-sigma) and the correlation threshold, $T_c = 0.70$. The T_v level was specified such that 30 percent of all SLPs were included in the analysis. After calculating the variation and correlation using Eqs. (1) and (2), the CSS is found from Eq. (3) to be CSS = $\{Sn_{5,13}, Sn_{5,14}, Sn_{5,15}S_{5,19}\}$. The location of the CSS elements is shown in Fig. 12.

Step (2) Problem Analysis

Task II Comparing Figs. 12, 7 and 4, one sees that all elements of the CSS are located on the Quarter Outer panel $C_{5,6}$. Therefore, following the diagnostic procedure presented in section 3.4, the Candidate Component is determined as $C^c_{5,6}$-Quarter Outer Panel.

Task III Since there is only one $C^c_{5,6}$ the Candidate Station is S^c_5 (Fig. 4).

Step (3) Root Cause Identification

Task IV In the symptom detection procedure described in section 3.3 there are two sub-tasks: (*1*) Estimation of the Vector of deformation and (*2*) estimation of the Area of deformation.

As shown in Fig. 12, all elements of the CSS are measurements along the *X* axis. Therefore, the direction of the Vector of deformation is along the *X* axis.

The Area of deformation is defined as the percentage of sensors localized in the $C^c_{5,6}$, which simultaneously belong to the CSS set. In this case, all sensors of $C^c_{5,6}$ (except $Sn_{5,16}$) are elements of CSS = $\{Sn_{5,13}, Sn_{5,14}, Sn_{5,15}, Sn_{5,19}\}$. The Area of deformation is spread throughout the whole $C^c_{5,6}$. Based on this analysis it can be concluded that this case depicts a *global symptom* in the X axis.

Task V The fact that the deformation is a *global symptom* in the *X* axis suggests some discrepancies in the PLP pin controlling the *X* direction in S^c_5 (Table 1). Based on the HG of PLPs (Fig. 6), the suggested root cause is the PLP pin $P_{5,3}(x,$

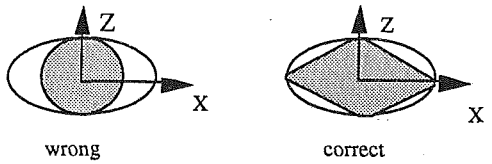

Fig. 13 PLP pin $P_{5,3}(x, z)$ before and after corrective action

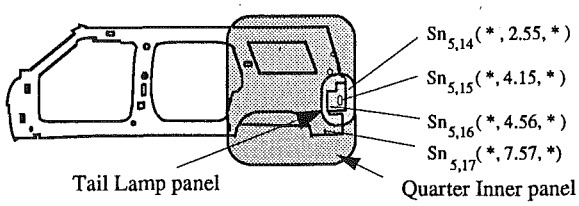

Fig. 14 Case study II-LH-APT scheme with marked elements of CSS set

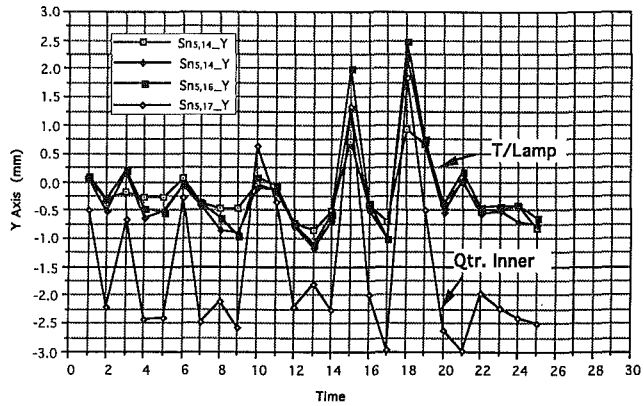

Fig. 15 X-bar chart for CSS = $\{Sn_{5,14}, Sn_{5,15}, Sn_{5,16}, Sn_{5,17}\}$

z), since, it is the only pin that controls the Quarter Outer in the X direction.

Step (4) Root Cause Verification and Performance Evaluation

Task VI After a detailed investigation of S_5^c, it was found that $P_{5,3}(x, z)$ actually controls only the Z direction due to incorrect design of the pin (Fig. 13). After corrective action was completed, the 6σ variation was reduced by approximately 20 percent for CSS sensors. Table 2 shows the 6σ variation for selected sensors before and after corrective action.

Case Study II: Tail Lamp Panel Dimensional Discrepancies. This case study illustrates the diagnostic of a fault pertaining to tooling installation.

(1) Problem Identification

Task I All constraints were the same as in case study I. After calculating the variation and correlation using Eqs. (1) and (2), the CSS is found from Eq. (3) to be CSS = $\{Sn_{5,14}, Sn_{5,15}, Sn_{5,16}, Sn_{5,17}\}$. The location of the CSS elements is shown in Fig. 14. Figure 15 shows X-bar charts for SLPs belonging to the CSS. All SLPs show strong correlation (Table 3).

(2) Problem Analysis

Task II Comparing Figs. 14, 7 and 4, one sees that all elements of the CSS are located on the Tail Lamp panel ($C_{5,7}$) and Quarter Inner panel ($C_{5,2}$). Based on Eq. (2), the Candidate Components are $C_{5,7}^c$ and $C_{5,2}^c$.

Task III The Candidate Station is determined to be the nearest station between the Candidate Components [Fig. 11(*a*)]. Based on Fig. 4, the Candidate Station is station S_3^c (the Inner & Outer Aperture marriage station).

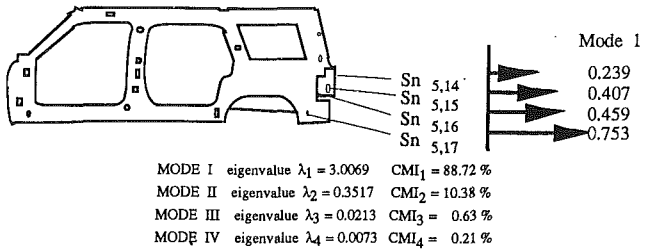

Fig. 16 Graphical representation of the eigenvector 1 (Vector 1)

Table 2 Evaluation of case study I

Sample of 100

Sensor	BEFORE	AFTER
	variation - 6-sigma	variation -6-sigma
$Sn_{5,14}$ X	3.76	2.87
$Sn_{5,13}$ X	2.85	2.47

Table 3 Correlation matrix

SAMPLE OF 100

	$Sn_{5,14}$	$Sn_{5,15}$	$Sn_{5,16}$	$Sn_{5,17}$
$Sn_{5,14}$	1.000			
$Sn_{5,15}$	0.943	1.000		
$Sn_{5,16}$	0.934	0.988	1.000	
$Sn_{5,17}$	0.800	0.835	0.834	1.000

Table 4 Eigenvectors associated with covariance matrix

	Vector 1	Vector 2
$Sn_{5,14}$	0.239	-0.273
$Sn_{5,15}$	0.407	-0.464
$Sn_{5,16}$	0.459	-0.526
$Sn_{5,17}$	0.753	0.658

(3) Root Cause Identification

Task IV The fault symptom is determined in the way described in section 3.3. Since all elements of the CSS show variation in the Y axis, the direction of the Vector of deformation is also the Y axis. The Area of deformation has a global character for the Tail Lamp (all sensors on the panel belong to CSS) and a local character for the Quarter Inner (only one sensor on the panel belongs to CSS). The Principal Component Analysis is used to determine the Vector of deformation. Calculating the two eigenvectors for four variables $\{Sn_{5,14}, Sn_{5,15}, Sn_{5,16}, Sn_{5,17}\}$, we get projections of the measurements from the 4-sensors of the CSS onto a 2-dimensional subspace. The first two eigenvectors are presented in Table 4. Figure 16 shows a geometric interpretation of Mode I (eigenvector 1).

Since the first eigenvector contributes 88.72 percent (Fig. 16) to the total variation, only the first eigenvector is considered in further analysis. The largest element of the first eigenvector for the CSS corresponds to sensor $Sn_{5,17}$, and decreases for sensors located "higher" ($+Z$ direction). This means that the source of the variation is approximately around sensor $Sn_{5,17}$.

Based on this analysis, it can be concluded that this case study has a *global symptom* in the Y direction for the Tail Lamp panel, and a *local symptom* in the Y direction for the Quarter Inner panel with the origin of deformation localized around sensor $Sn_{5,17}$.

Task V Using the rules described in Table 1, it is suggested that the root cause might be external interference or discrepancy related to the WLPs around sensor $Sn_{5,17}$, occurring in

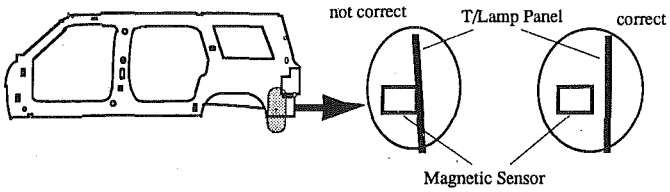

Fig. 17 Mechanism of fault occurrence in case study II

Table 5 Evaluation for case study II

Sample of 100

Sensors	Before 6-σ [mm]	After 6-σ [mm]
$Sn_{5,14}$	2.63	1.32
$Sn_{5,15}$	4.08	1.67
$Sn_{5,16}$	3.98	1.99
$Sn_{5,17}$	5.64	2.12

S_3^c. However, the HG of WLPs contains no WLP around sensor $Sn_{5,17}$. Thus, the final suggestion is that the external interference near sensor $Sn_{5,17}$ in the Quarter Inner panel occurred in station S_3^c.

(4) Root Cause Verification and Performance Evaluation

Task VI After investigation of station S_3^c, interference between the magnetic sensor (part-present-sensor) and the Quarter Inner panel was discovered. The magnetic sensor was installed too close to the panel, causing interference with the panel near $Sn_{5,17}$ (Fig. 17).

After the magnetic sensor was relocated, the deformation of the Quarter Inner panel was eliminated. Table 5 shows the 6-sigma variation of the measurements before and after correction.

5 Summary and Conclusions

The launch of an auto-body assembly process is an important stage of the vehicle development cycle. An efficient approach to process diagnostic during launch is beneficial not only for overall cost reduction and quality improvement, but also to provide quick feedback with suggestions for the design of a new product or process.

This paper is the first attempt to develop a knowledge-based diagnostic approach for the launch of an auto-body assembly process. The proposed knowledge-based solution for diagnosis makes this approach more flexible during implementation for launching different auto-body assembly processes with different product, process and measurement points. In this paper the knowledge representation and a diagnostic reasoning mechanism are proposed.

The knowledge representation is based on the functional characteristics of the product, tooling, process, and measurements, which are in turn defined as collections of hierarchical groups. The hierarchical groups explicitly show the relationship between the most important features of auto-body assembly. A major advantage of the proposed knowledge representation is that a great deal of knowledge can be represented within a unified framework. This unified framework allows easy access to and fast diagnostic reasoning for root causes of faults. In addition, no presolved cases are necessary to create the knowledge base, which makes this approach a viable strategy for the launch period.

The diagnostic reasoning includes five major tasks: (*i*) selection of the Candidate Set of Sensors (CSS), (*ii*) determination of the Candidate Components, (*iii*) determination of the Candidate Station, (*iv*) fault symptom detection and (*v*) root cause detection. The fault symptom detection procedure determines the direction and area of the panel deformation. Fault root cause identification uses general rules to determine potential root causes of faults in the assembly line.

Two case studies were presented to illustrate the proposed diagnostic approach. The results showed significant performance improvement after implementing this approach. In one domestic assembly plant the dimensional variation of the auto-body during the launch period was reduced by 250 percent to a level no other US automobile manufacturer has ever achieved.

Acknowledgment

This work was partially funded by NSF—Industry/University Cooperative Research Center for Dimensional Measurement and Control in Manufacturing.

We are thankful to those reviewers whose comments helped improve this paper.

References

Becker, L. A., Bartlet, R., Kinigadner, A., Roy, M., 1989, "Using Manufacturing Process Representations," *Journal of Artificial Intelligence for Engineering Design, Analysis and Manufacturing* (*AI EDAM*), Vol. 3, pp. 23–34.

Buchanan, B. G., and Shortliffe, E. H., eds., 1984, *Rule-Based Expert Systems: The MYCIN Experiments of the Stanford Heuristic Programming Project*, Addison-Wesley, Reading, MA.

Buchanan, B. G., and Feigenbaum, E. A., 1978, "Dendral and Meta-Dendral," *Artificial Intelligence*, Vol. 11, No. 1, pp. 5–24.

Chandrasekaran, B., and Goel, A., 1988, "From Numbers to Symbols to Knowledge Structures: Artificial Intelligence Perspectives on the Classification Task," *IEEE Trans. on Systems, Man, and Cybernetics*, Vol. 18, No. 3, pp. 415–424.

Chou, Y.-C., 1992, "A Theoretical Framework for Automatic Layout of Machining Fixtures," *Journal of Artificial Intelligence for Engineering Design, Analysis and Manufacturing* (*AI EDAM*), Vol. 6, pp. 111–121.

Dessouky, M. I., Kapoor, S. G., and DeVor, R. E., 1987, "A Methodology for Integrated Quality System," ASME JOURNAL OF ENGINEERING FOR INDUSTRY, Vol. 109, pp. 241–247.

Dooley, K. J., and Kapoor, S. G., 1990a, "An Enhanced Quality Evaluation System for Continuous Manufacturing Processes, Part 1: Theory," ASME JOURNAL OF ENGINEERING FOR INDUSTRY, Vol. 112, pp. 57–62.

Dooley, K. J., and Kapoor, S. G., 1990b, "An Enhanced Quality Evaluation System for Continuous Manufacturing Processes, Part 2: Application," ASME JOURNAL OF ENGINEERING FOR INDUSTRY, Vol. 112, pp. 63–68.

Gomez, F., and Chandrasekaran, B., 1981, "Knowledge Organization and Distribution for Medical Diagnosis," *IEEE Trans. on Systems, Man, and Cybernetics*, Vol. 11, No. 1, pp. 34–42.

Hu, S., and Wu, S. M., 1992, "Identifying Root Causes of Variation in Automobile Body Assembly Using Principal Component Analysis," *Trans. of NAMRI*, Vol. XX, pp. 311–316.

Isermann, R., and Freyermuth, B., 1991, "Process Fault Diagnosis Process Model Knowledge, Part I & II," ASME *Journal of Dynamic Systems, Measurement and Control*, Vol. 113, pp. 620–633.

Jolliffe, I. T., 1972, "Discarding Variables in a Principal Component Analysis, I: Artificial Data," *Applied Statistics*, Vol. 21, pp. 160–173.

Jolliffe, I. T., 1986, *Principal Component Analysis*, Springer-Verlag, New York.

Lu, S. C.-Y., and Tcheng, D. K., 1991, "Building Layered Models to Support Engineering Decision Making: A Machine Learning Approach," ASME JOURNAL OF ENGINEERING FOR INDUSTRY, Vol. 113, pp. 1–9.

Narayanan, N. H., and Viswanadham, N., 1987, "A Methodology for Knowledge Acquisition and Reasoning in Failure Analysis of Systems," *IEEE Trans. on Systems, Man, and Cybernetics*, Vol. 17, No. 2, pp. 274–288.

Scarl, E. A., Jamieson, J. R., and Delaune, C. I., 1987, "Diagnosis and Sensor Validation through Knowledge of Structure and Function," *IEEE Trans. on Systems, Man, and Cybernetics*, Vol. 17, No. 3, pp. 360–368.

Schwarz, S. A., and Lu, S. C-Y., 1992, "Representation, Acquisition, and Manipulation of Probabilistic Attribute Values to Support Engineering Decision Making," *Trans. of NAMRI*, Vol. XX, pp. 261–267.